Repurposing Poly(3-hexylthiophene) as a Conductivity-Reducing Additive for Polyethylene-Based High-Voltage Insulation

ADVANCED MATERIALS
www.advmat.de

Repurposing Poly(3-hexylthiophene) as a Conductivity-Reducing Additive for Polyethylene-Based High-Voltage Insulation

Amir Masoud Pourrahimi, Sarath Kumara, Fabrizio Palmieri, Liyang Yu, Anja Lund, Thomas Hammarström, Per-Ola Hagstrand, Ivan G. Scheblykin, Davide Fabiani, Xiangdong Xu, and Christian Müller**

Poly(3-hexylthiophene) (P3HT) is found to be a highly effective conductivity-reducing additive for low-density polyethylene (LDPE), which introduces a new application area to the field of conjugated polymers. Additives that reduce the direct-current (DC) electrical conductivity of an insulation material at high electric fields have gained a lot of research interest because they may facilitate the design of more efficient high-voltage direct-current power cables. An ultralow concentration of regio-regular P3HT of 0.0005 wt% is found to reduce the DC conductivity of LDPE threefold, which translates into the highest efficiency reported for any conductivity-reducing additive to date. The here-established approach, i.e., the use of a conjugated polymer as a mere additive, may boost demand in absolute terms beyond the quantities needed for thin-film electronics, which would turn organic semiconductors from a niche product into commodity chemicals.

1. Introduction

Poly(3-hexylthiophene) (P3HT) is one of the most widely studied conjugated polymers that has received a tremendous amount of attention for a wide range of applications from flexible electronics to photovoltaics and thermoelectrics.[1] Conjugated polymers such as P3HT are used as semiconductors or conductors that compete head-on with other types of materials, e.g., with metal halide perovskites or amorphous silicon in case of photovoltaics,[2] and carbon allotropes or metals in case of wearable electronics.[3] As a result, despite of continuing research efforts the widespread commercial use of P3HT, and in fact conjugated polymers in general, is yet to emerge.

One intriguing alternative is the use of conjugated polymers in combination with a commodity polymer such as polyethylene, polystyrene, or poly(ethylene oxide). The commodity polymer not only dilutes the typically more expensive conjugated polymer but also enhances its environmental stability and imparts superior mechanical properties. In some cases only a relatively small amount of the conjugated polymer (2–20 wt%) is needed in order to achieve the desired degree of electronic or electrical functionality, e.g., when used for the fabrication of organic field-effect transistors (FETs)[4–7] and solar cells[8,9] or as a thermoelectric material.[10,11] Yet again, previous reports that deal with semiconductor:insulator blends treat the conjugated polymer as the principal ingredient, whereas the commodity polymer only takes on an auxiliary role as a binder material. Polymers like P3HT may find their unique niche application once they are instead used as an additive, while the commodity polymer remains the key component.

Here, we establish that P3HT can be used as a potent conductivity-reducing additive for polyethylene, which improves the insulation properties of the commodity polymer. A good insulation material, such as those that are to be used to insulate high-voltage direct-current (HVDC) power cables, must feature a very low direct-current (DC) electrical conductivity. HVDC cables are essential for the seemless integration of renewable sources of energy into future power grids.[12,13] Therefore, considerable academic research efforts are currently dedicated

Dr. A. M. Pourrahimi, Dr. L. Yu, Dr. A. Lund, Prof. C. Müller
Department of Chemistry and Chemical Engineering
Chalmers University of Technology
Göteborg 41296, Sweden
E-mail: amirmas@chalmers.se; christian.muller@chalmers.se

Dr. S. Kumara, Dr. T. Hammarström, Dr. X. Xu
Department of Electrical Engineering
Chalmers University of Technology
Göteborg 41296, Sweden

Dr. F. Palmieri, Prof. D. Fabiani
Department of Electrical, Electronic, and Information Engineering
University of Bologna
Bologna 40136, Italy

Dr. P.-O. Hagstrand
Innovation & Technology
Borealis AB, Stenungsund 44486, Sweden

Prof. I. G. Scheblykin
Chemical Physics and NanoLund
Lund University
PO Box 118, Lund 22100, Sweden

The ORCID identification number(s) for the author(s) of this article can be found under https://doi.org/10.1002/adma.202100714.

DOI: 10.1002/adma.202100714

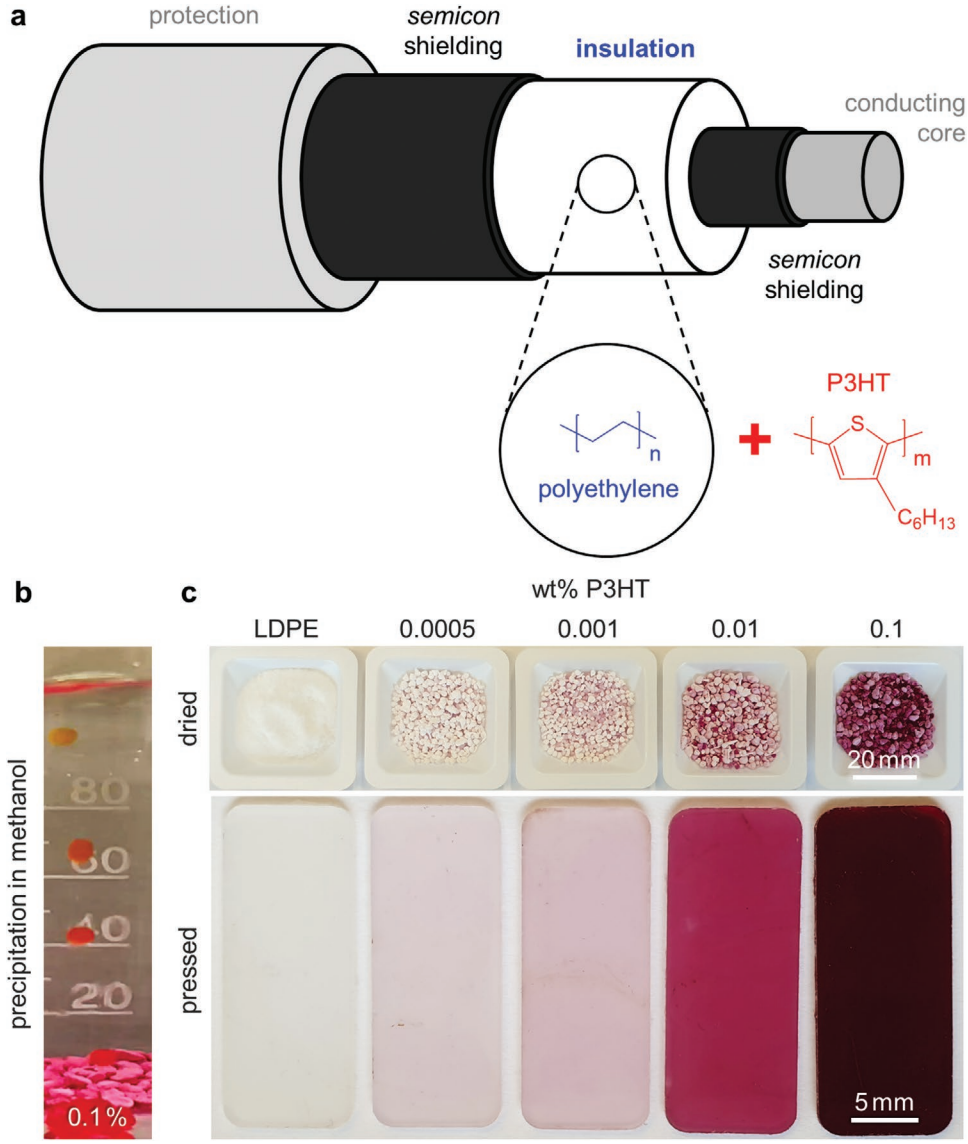

Figure 1. Schematic of a HVDC cable and preparation of P3HT:LDPE blends. a) Basic layout of an extruded HVDC power cable consisting of a conducting core (Al or Cu), surrounded by "semicon" layers (a carbon black composite), the extruded insulation layer, and outer protection layers (outer covering/sheat). b,c) Photograph of drops of a 0.1 wt% P3HT:LDPE blend dissolved in *p*-xylene during precipitation in methanol (b), and dried precipitate with different P3HT contents (top) that was subsequently melt-pressed (bottom; sample thickness = 1 mm) (c).

to the development of additive concepts that allow to further reduce the DC conductivity of polymeric insulation materials,[14] which may facilitate the design of HVDC cables that incur lower transmission losses.

Additives that have been shown to reduce the DC conductivity of low-density polyethylene (LDPE), the most widely used insulating material for the manufacture of extruded HVDC cables (see **Figure 1** for the basic layout of a power cable), include higher-melting polyethylenes,[15] metal oxide nanoparticles,[16–20] carbon allotropes,[21,22] and various aromatic molecules[23–25] (**Table 1**). These additives are thought to function as trapping sites for charge carriers that lower the charge-carrier mobility[14] and hence reduce the electrical conductivity by up to 300 times in case of 3 wt% of ZnO nanoparticles.[16] This approach is contrary to the concept of trap-filling in case of opto-electronic devices, such as FETs and solar cells through molecular doping,[26,27] which has the purpose to enhance and not hinder charge conduction. It is typically necessary to add several weight percent of the above-mentioned conductivity-reducing additive in order to notably lower the conductivity, which tends to result in aggregation during compounding. A comparison of the recent literature reveals that the efficiency of conductivity-reducing additives, which we here define as $\eta = (\sigma_{DC}^{PE}/\sigma_{DC})/\phi$, where ϕ is the weight percent (wt%) of the additive, reaches a value of up to $\eta \approx 100$ and 700 wt%$^{-1}$ in the case of ZnO nanoparticles and graphene oxide, respectively (Table 1). A conductivity-reducing additive that achieves the desired function at a very low concentration would constitute a significant advantage since it does not unduly compromise the cleanliness of the insulation material. We find that an ultralow

Table 1. Effect of different types of conductivity-reducing additives on the DC conductivity of LDPE expressed in terms of the DC conductivity σ_{DC} of the additive-containing resin relative to the DC conductivity of the neat LDPE resin σ_{DC}^{PE} (absolute values reported in Table S1, Supporting Information), and as the efficiency $\eta = (\sigma_{DC}^{PE}/\sigma_{DC})/\phi$, where ϕ is the additive content in wt%. The survey is limited to DC conductivity measurements where the electric field was applied for at least 1 h, although values approaching the steady-state are only obtained for much longer measurements[28].

	Type of additive	ϕ [wt%]	E (kV mm^{-1})	T [°C]	t [h]	$\sigma_{DC}^{PE}/\sigma_{DC}$	η [wt%$^{-1}$]	Ref.
Inorganic nanoparticles	ZnO	3	32.5	60	11	300	100	[16]
	MgO	3	32.5	60	11	54	18	[17]
	Al_2O_3	3	32.5	60	11	30	10	[18]
	SiO_2	2	40	25	1	8	4	[19]
Polyolefins	HDPE[a)]	1	30	70	24	13	13	[15]
Hybrid	HDPE +Al_2O_3	4 + 3	32	70	6	333	48	[20]
Carbon allotropes	Graphene	0.1	20	25	2	9	90	[21]
	Graphene	0.1	20	70	2	2	20	[21]
	Graphene oxide[a)]	0.01	40	90	4	7	700	[22]
Aromatic molecules	Anthracene	0.5	10	60	1.5	5	10	[23]
	3-Aminobenzoic acid[a)]	1	50	70	1	18	18	[24]
	4,4′-Dihydroxy benzophenone	0.5	10	70	12	5	10	[25]
Conjugated polymers	P3HT	0.0005	50	70	12	3	6000	This work

[a)]The matrix is crosslinked LDPE (XLPE).

concentration of 0.0005 wt% P3HT (5 ppm) reduces the DC conductivity of LDPE approximately threefold, which yields a record conductivity-reducing efficiency of $\eta \approx 6000$ wt%$^{-1}$ (Table 1).

2. Results and Discussion

To prepare blends of LDPE and regioregular P3HT, we dissolved and mixed the two polymers in *p*-xylene at 100 °C, followed by dropwise precipitation in methanol at 0 °C (Figure 1b). The dried precipitate was subsequently melt-pressed at 150 °C, i.e., above the melting temperature of LDPE, $T_m^{LDPE} \approx 110$ °C, but far below $T_m^{P3HT} \approx 250$ °C to avoid degradation (Figure S1, Supporting Information). Melt-pressed plaques with a thickness of 0.7 mm appeared homogeneous and had a pale pink to dark magenta color depending on the P3HT content (Figure 1c). The faint color of blends with a P3HT content $c_{P3HT} \leq 0.01$ wt% bodes well for industrial use where visual inspection of a polyolefin is widely used for quality control.

To assess the degree of compatibility of the two polymers, we carried out a series of differential scanning calorimetry (DSC) experiments to determine the peak melting temperatures of the two components as a function of blend composition (Figure S2, Supporting Information). For blends with $c_{P3HT} \geq 5$ wt%, the peak melting temperature of both components (extracted from second heating DSC thermograms) is largely unaffected by the presence of the second polymer. However, for $c_{P3HT} < 5$ wt%, a gradual decrease in T_m^{P3HT} occurred (**Figure 2**). For the composition range of $c_{P3HT} = 0.01$–1 wt%, DSC experiments were complemented with a visual inspection of melt-pressed samples (0.1 and 0.3 mm thickness for c_{P3HT} above and below 0.1 wt%, respectively) that experienced a temperature gradient, which was created by placing samples on a Kofler bench (Figure S3, Supporting Information). A change in color from purple to orange/yellow indicated melting of P3HT, which was used as an indicator for T_m^{P3HT}. We were able to confirm that T_m^{P3HT} gradually decreases as the P3HT content is reduced. This trend can be explained with partial miscibility of the conjugated polymer with molten LDPE, which is comparable to the phase behavior of P3HT and HDPE.[4] To support that the observed decrease in T_m^{P3HT} arises due to partial miscibility and not merely a decrease in crystal size we placed a grain of P3HT onto a 30 µm thick sheet of LDPE and heated the materials for 2 min at 250 °C (Figure S4, Supporting Information). The distinct purple halo that develops around the P3HT grain indicates that the conjugated polymer readily diffuses into LDPE, which confirms that the two materials are partially miscible.

A binary (nonequilibrium) temperature-composition phase diagram of P3HT and LDPE was constructed to summarize the monotectic phase behavior of this blend (Figure 2a). For blends $c_{P3HT} > 5$ wt%, we deduce that the liquid state comprises a phase-separated melt denoted $L_1 + L_2$, which upon cooling first undergoes solidification of P3HT and then LDPE, forming a phase-separated solid denoted $S_{LDPE} + S_{P3HT}$ below T_m^{LDPE}. Instead, for sufficiently low concentrations of P3HT, i.e., $c_{P3HT} < 5$ wt%, there exists a homogeneous phase L_1 above T_m^{LDPE} where the conjugated polymer is dissolved in molten LDPE. During cooling of blends with $c_{P3HT} \approx 0.01$–2 wt%, which is the thermal history experienced during melt-pressing (cf. above and Experimental), the conjugated polymer gradually solidifies as its solubility in molten LDPE decreases with temperature, resulting in a fine distribution of P3HT in LDPE.

We were interested in determining the extent to which P3HT is able to aggregate upon solidification for $c_{P3HT} < 1$ wt%. A UV–vis absorption spectrum recorded for $c_{P3HT} = 0.01$ wt% shows a pronounced shoulder at 600 nm, which indicates π–π stacking of P3HT (Figure S5, Supporting Information). For $c_{P3HT} < 5$ wt% individual polymer chains are dissolved in phase L_1, which however aggregate, possibly with themselves,

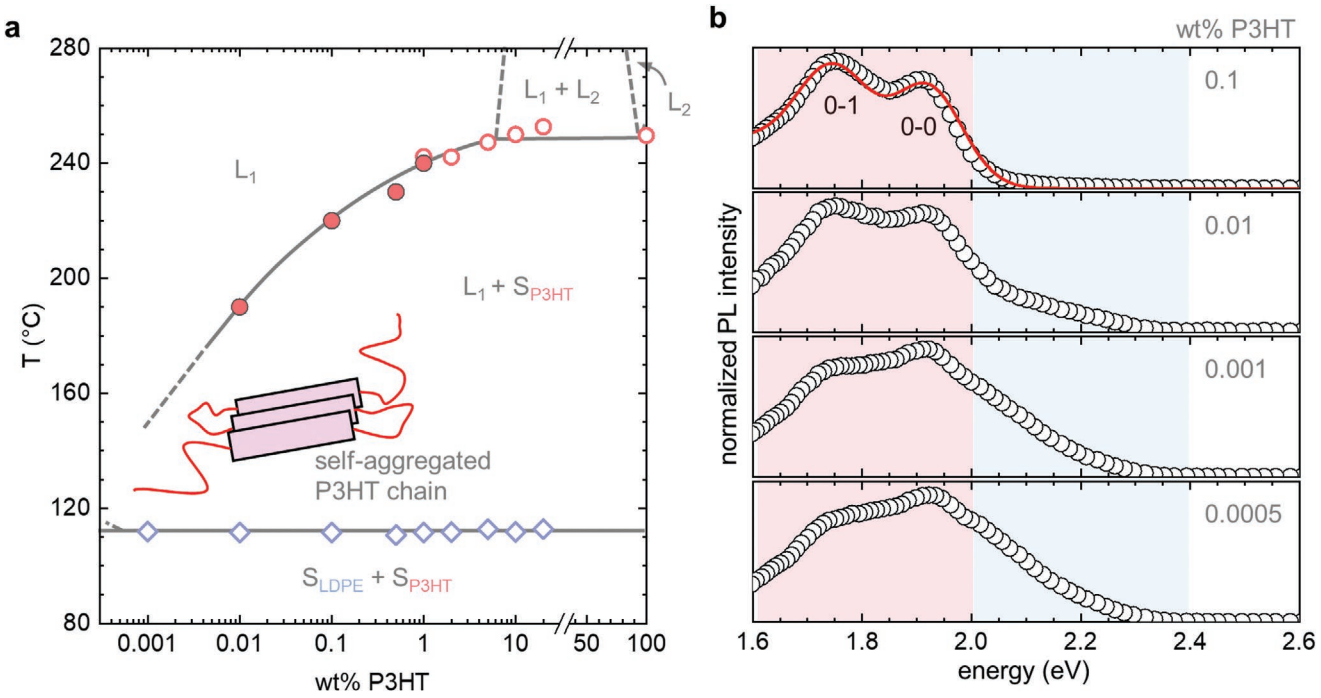

Figure 2. Monotectic phase behavior of P3HT:LDPE. a) Temperature–composition phase diagram of P3HT:LDPE constructed with peak melting temperatures extracted from DSC second-heating thermograms (P3HT: open circles; LDPE: open diamonds) and visual inspection of thin films that experience a temperature gradient on a Kofler bench (filled circles; estimated error ±5–10 °C; note the excellent agreement of T_m^{P3HT} for c_{P3HT} = 1 wt% determined using DSC or the Kofler bench); L_1 and L_2 denote LDPE- and P3HT-rich liquid phases, respectively, while S_{LDPE} and S_{P3HT} indicate solid LDPE and P3HT. b) Photoluminescence (PL) spectra of P3HT:LDPE blends with $c_{P3HT} \leq 0.1$ wt%, as well as a fit using the modified Franck–Condon model from Spano et al.[29,30] (red solid line); the red and blue shaded areas indicate the range of energies where aggregated and nonaggregated P3HT emit, respectively.

upon solidification (cf. Figure 2). Since it was not possible to record UV–vis spectra for lower P3HT contents because of the low optical density of our samples and scattering by the polyethylene matrix, we also carried out photoluminescence (PL) spectroscopy (Figure 2b). The PL spectrum recorded for c_{P3HT} = 0.1 wt% can be fitted with the modified Frank–Condon model from Spano et al.[29,30] (Figure 2b top; and Figure S6, Supporting Information), indicating that the conjugated polymer behaves similar to neat P3HT in the absence of LDPE. For this composition P3HT is able to strongly phase-separate during solidification, resulting in P3HT-rich domains that show classical aggregation behavior. PL spectra recorded for blends with $c_{P3HT} \leq 0.01$ wt% have a markedly different shape with a new emission band emerging above 2 eV (Figure 2b). Emission at higher energies can be assigned to nonaggregated polymer chains,[31,32] as argued for instance by Dyson et al. for a polythiophene with tetraethylene glycol side chains blended with poly(ethylene oxide).[33] For the lowest measured composition of c_{P3HT} = 0.0005 wt% the PL emission spectrum shows both features of aggregated and nonaggregated P3HT. It can be concluded that the conjugated polymer partially aggregates even at low compositions $c_{P3HT} < 0.01$ wt%, which approach the monotectic composition, albeit likely as a single, self-aggregated chain due to the high degree of dilution in LDPE.

We went on to determine the DC electrical conductivity of P3HT:LDPE blends, and chose to focus on blends with $c_{P3HT} \leq$ 0.1 wt% for which the semiconductor content is sufficiently dilute to minimize the likelihood of percolation. Melt-pressed films with a thickness of ≈0.1 mm were placed between two planar electrodes and the whole setup was positioned in an oven in order to maintain a well-defined temperature (**Figure 3**a). A stepwise increasing electric potential was applied to the high-voltage electrode, which generated an electric field that stepwise increased from 10 to 50 kV mm^{-1} (Figure 3b; and Figure S7a, Supporting Information). The charging current (leakage current) was recorded at each electric field. In the case of neat LDPE, we compared three measurements using two different setups as well as different processing protocols (melt-pressing of precipitated material vs as-received pellets), which yielded comparable charging currents at 70 °C (Figure S7b, Supporting Information), indicating a high degree of reproducibility.

Initially, we were interested in screening blend compositions up to c_{P3HT} = 0.1 wt% and therefore selected a relatively short duration of 3 h for each charging step (Figure S7c, Supporting Information). For c_{P3HT} = 0.01 and 0.1 wt%, we observe a marked increase in charging current compared to neat LDPE at 70 °C, which indicates that the P3HT additive starts to improve charge transport at these compositions, i.e., the semiconductor forms a percolating network. Instead, for $c_{P3HT} < 0.01$ wt%, no increase in charging current occurred, and therefore we chose to carry out a more in-depth analysis of blends with c_{P3HT} = 0.0005 and 0.001 wt%. To minimize any contribution by residual polarization or space-charge limited current,[34] a duration of 12 h per charging step was

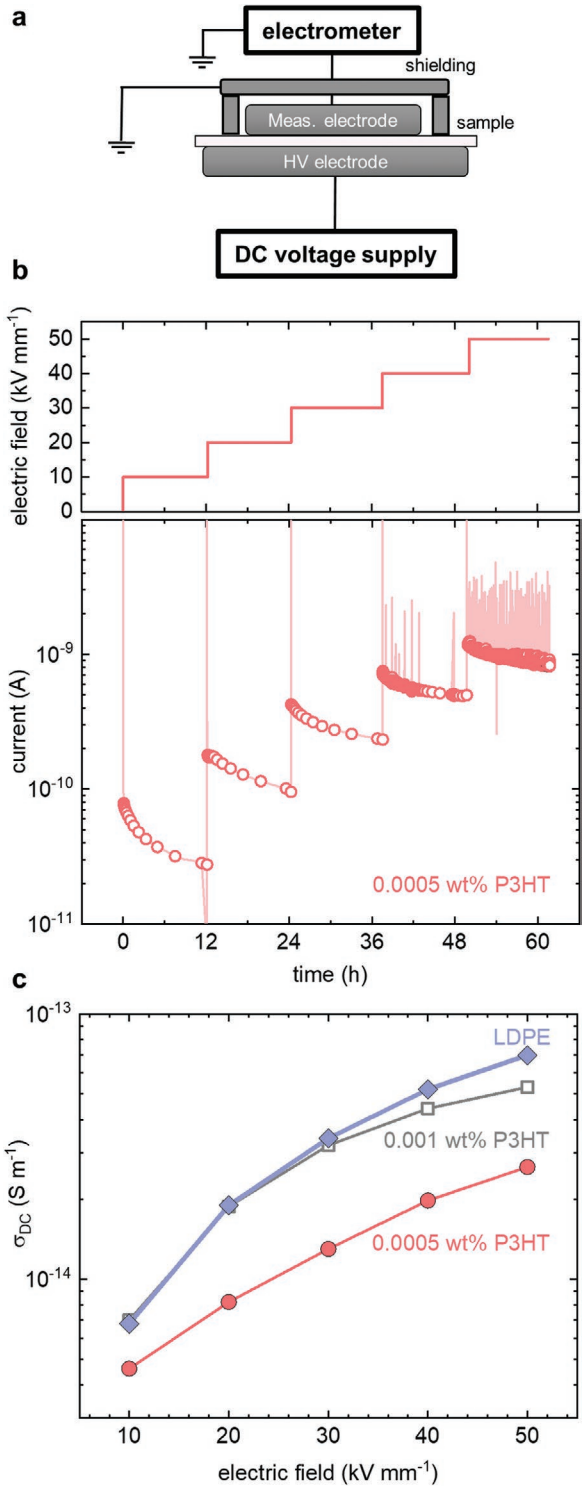

Figure 3. High-voltage DC conductivities σ_{DC} of P3HT:LDPE blends measured for ≈0.1 mm thick plaques at 70 °C. a) The three-electrode measurement setup comprising the sample sandwiched between two electrodes and sourrounded by a shielding (guard) electrode. b) The applied step-wise electric field (top) and the charging current in the samples (bottom) as a function of time; the σ_{DC} values are calculated based on the charging current at the end of each 12 h step. c) σ_{DC} as a function of the applied electric field for neat LDPE (blue) and blends with c_{P3HT} = 0.001 wt% (gray) and 0.0005 wt% (red).

chosen. The charging current at 30 °C was recorded, while stepwise increasing the electric field from 10 to 50 kV mm^{-1} (Figure S8, Supporting Information), and then the same protocol was repeated at 70 °C (Figure 3b). The DC conductivity was calculated based on the current measured at the end of each 12 h charging step (Figure 3c; and Figure S8, Supporting Information). We observe a significantly lower σ_{DC} for both studied compositions at 30 °C, while at 70 °C in particular c_{P3HT} = 0.0005 wt% yields a lower DC conductivity (a lower P3HT content of c_{P3HT} = 0.0001 wt% did not alter the DC conductivity; not shown). For instance, for c_{P3HT} = 0.0005 wt%, we obtain $\sigma_{DC} \approx 8 \times 10^{-15}$ S m^{-1} at 20 kV mm^{-1} and 70 °C in contrast to neat LDPE, which displays a significantly higher $\sigma_{DC} \approx 2 \times 10^{-14}$ S m^{-1} at the same conditions.[35] This corresponds to a remarkably high conductivity-reducing efficiency of $\eta \approx 5000$ wt%$^{-1}$, which increases to 6000 wt%$^{-1}$ at 50 kV mm^{-1}. It can be anticipated that a higher absolute reduction in conductivity could be achieved if it was possible to add more P3HT while avoiding the onset of percolation (cf. Figure S7c, Supporting Information), for example by adjusting the regioregularity and molecular weight of the conjugated polymer.

In a further set of experiments, the distribution of space charge was determined because we were concerned that the P3HT additive leads to accumulation of charges, which would increase the probability of breakdown. Pulsed electroacoustic analysis (PEA) was carried out to visualize the microscale space charge distribution. Melt-pressed plaques with a thickness of ≈0.1 mm were placed between two planar electrodes (upper electrode: semiconductive, diameter 10 mm; lower electrode: aluminum plate), and the setup was heated in an oven to 70 °C. The charge distribution was monitored while polarizing the sample at a constant electric field of 50 kV mm^{-1} for 3 h, followed by a 1 h long discharging step after removal of the electric field (**Figure 4**; and Figure S9, Supporting Information).

Neat LDPE displays a type of behavior that is typical for a good high-voltage insulation material. Homo-charges (i.e., charges that have the same polarity as the electrodes)[36] are injected upon application of the electric field, as evidenced by peaks in the charge density with the same polarity as the respective electrode at either surface of the plaque, while the build-up (accumulation) of charge in the bulk of the material is minimal (cf. Figure 4a). Further, the space charge distribution was stable during the whole polarization step. Once the electric field is removed the charge across the LDPE plaque immediately dissipates, which suggests that no significant amount of hetero-charge (i.e., charges in the form of ionized impurities)[36] accumulate in the material. Gratifyingly, blends with an ultralow content of P3HT display charging and discharging behavior that is comparable to neat LDPE (Figure 4b; and Figure S10, Supporting Information). A concentration of c_{P3HT} = 0.0005 or 0.001 wt% does not appear to increase charge accumulation. In contrast, for c_{P3HT} = 0.01 wt% a markedly different behavior is observed. There is a significant build-up of charge in the bulk of the sample during polarization at 50 kV mm^{-1}, and once the electric field is removed a considerable amount of charge remains even one hour into the discharge step, indicating the presence of hetero-charges that have accumulated in the material.[14,37]

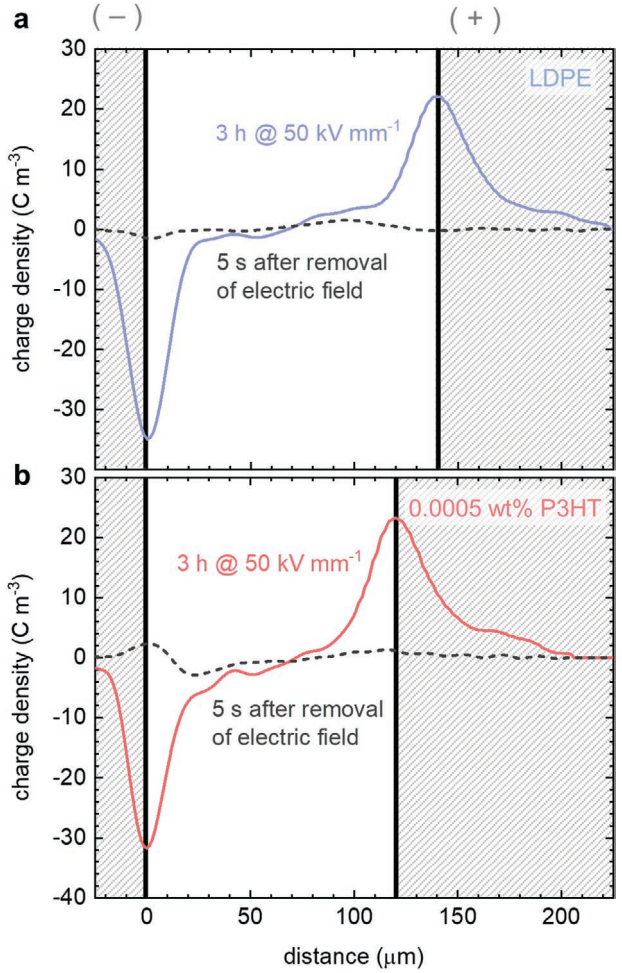

Figure 4. a,b) Space charge distribution at 70 °C across plaques of LDPE (a) and P3HT:LDPE with c_{P3HT} = 0.0005 wt% (b), that have experienced an electric field of 50 kV mm^{-1} for 3 h (solid lines) and 5 s after removal of the electric field (dashed lines); the electrodes and thickness of the plaques are indicated with hatched and white areas, respectively.

Although PEA is illustrative for the charge distribution in the bulk, its spatial resolution is low, and therefore one cannot distinguish between the capacitive charge on the sample/electrode interface and charges trapped just below the sample surface. Hence, PEA was complemented with isothermal surface potential decay (ISPD) measurements at 70 °C, which allow detection of trapped charges in the subsurface regions.[38] PEA provides information about the dissipation of the "total absolute charge density"[39] (not net charge) during the discharge step (Figure S11a, Supporting Information), while ISPD monitors the dissipation of surface potential (Figure S11b, Supporting Information). Neat LDPE and blends with c_{P3HT} = 0.0005 and 0.001 wt% display a similar PEA transient but feature lower initial surface potentials as well as a faster decay of the surface charge. It is feasible that the addition of an ultralow content of P3HT reduces the probability for charge trapping in a subsurface region close to the electrodes while trapping in the bulk of the material becomes more likely. Instead, for c_{P3HT} = 0.01 wt% the total charge that remains during the discharge step increases by close to one order of magnitude, as compared to neat LDPE (Figure S11, Supporting Information). In contrast, the surface potential as measured with ISPD is considerably lower, which is consistent with a higher bulk conductivity facilitated by a percolating network of the P3HT additive.

3. Conclusions

The addition of an ultralow content $c_{P3HT} \leq 0.001$ wt%, i.e., less than 10 ppm, of the conjugated polymer P3HT to LDPE can reduce the DC electrical conductivity by a factor of up to 3 and does not enhance the accumulation of space charge. Evidently, P3HT is an effective conductivity-reducing additive with an efficiency η of up to 6000 wt%$^{-1}$, which far exceeds the efficiency of any other compound that has been investigated to date. The exceptionally low amount of P3HT that is required may pave the way for the design of insulation materials with an ultralow DC electrical conductivity. It can be anticipated that optimization of the molecular weight and regioregularity of P3HT will result in an even stronger reduction in conductivity. The manufacture of a 100 km long HVDC cable with a 6 cm wide conducting core surrounded by a 3 cm thick insulation layer would require about 4 kg of P3HT, assuming c_{P3HT} = 0.0005 wt%, which would in due time considerably boost the availability of the conjugated polymer. Repurposing conjugated polymers as an additive for polyolefins, rather than employing them as the active material in optoelectronic devices, may considerably enhance the scope of this promising class of materials.

4. Experimental Section

Materials: LDPE ($M_n \approx$ 21 kg mol^{-1}, PDI ≈ 6, and number of long-chain branches ≈ 1.9 determined with SEC using an Agilent PL-GPC 220 system) was obtained from Borealis AB and P3HT ($M_n \approx$ 91 kg mol^{-1}, PDI ≈ 1.8, regioregularity ≈93%) was obtained from Sungyoung Ltd. LDPE (100 g L^{-1}) and P3HT (0.05 to 2 g L^{-1}) were each dissolved in *p*-xylene (anhydrous, purity ≥ 99%, Sigma-Aldrich) at 100 °C. The polymer solutions were mixed to obtain the desired P3HT:LDPE ratio, including neat LDPE, followed by dropwise precipitation in methanol (analytical grade, purity ≥ 99.9%, Fisher Chemical) at 0 °C. The precipitate was collected with a filter, rinsed two times with pure methanol, and finally dried in a vacuum oven at 60 °C and air pressure of 20 kPa overnight. Plaques with a thickness of 0.1–1 mm were melt-pressed at 150 kN force (3.75 MPa) at 150 °C, followed by cooling to room temperature at about 10 °C min^{-1}.

Thermal Analysis: DSC was carried out with a DSC2 from Mettler Toledo under nitrogen (50 mL min^{-1}), between −50 and 150 °C (for the first heating and cooling) and −50 and 300 °C at (for the second heating), at a scan rate of 10 °C min^{-1}. The sample weight was ≈2 mg. For visual determination of P3HT melting, melt-pressed samples (area ≈10 × 150 mm^2, thickness ≈0.1 or 0.3 mm) on glass slides were placed on a Kofler bench from Wagner & Munz.

UV–Vis Absorption Spectroscopy: UV–vis spectra of melt-pressed plaques were recorded with a Lambda 1050 spectrophotometer from PerkinElmer.

PL Spectroscopy: PL spectra of 0.1 mm thick samples, which were excited at 514 nm (CW Ar-ion laser), were recorded with a universal fluorescence microspectroscopy platform based on Olympus IX-71 microscope described elsewhere.[40]

High-Voltage DC Conductivity Measurements: Melt-pressed plaques with a thickness of ≈0.1 mm were sandwiched between two planar electrodes (see Figure 3a). The high-voltage (HV) and measuring (Meas.)

electrodes had a diameter of 60 mm and 28 mm, respectively. A third shielding electrode was used as a guard to divert any influence of surface to ground currents. The setup was placed in a shielded oven (Memmert UN30). One electrode was grounded via a Keithley 6517B electrometer, while a potential of ≈1–5 kV was applied to the high-voltage electrode using a DC voltage supply (Glassman FJ60R2, 60 kV, 2 mA), resulting in an electric field of 10–50 kV mm^{-1}. The volume leakage current was measured with the electrometer followed by dynamic averaging.[41] To filter out high-frequency noise, a low-pass filter was added to the circuit at the high-voltage side. The DC conductivity was calculated according to $\sigma_{DC} = id/UA$ where i, U, A, and d are charging current at the end of each charging step, applied potential, area of the measuring electrode and thickness of the melt-pressed plaque. The reported σ_{DC} values have an error of ±4%, based on a comparison of three LDPE samples.[35]

PEA: Melt-pressed plaques with a thickness of ≈0.1 mm were wrapped in aluminum foil were allowed to discharge during storage at 60 °C in a vacuum oven for 1 day. Samples were then placed between two electrodes, the upper electrode was a semiconductive cylinder of 10 mm diameter, and the lower electrode an aluminum plane, and the setup was placed in an oven. PEA measurements were carried out by applying voltage pulses with an amplitude of 500 V and a width of 10 ns to the sample with a repetition rate of 110 Hz through a ceramic coupling capacitor of 220 pF. The charge density profile was extracted from the measurement signal coming from the piezoelectric sensor, once calibrated and deconvolved. Details on the PEA measurement principles can be found.[42] Samples were first polarized at an electric field of 50 kV mm^{-1} for 3 h and then depolarized for 1 h after removal of the electric field (discharging).

ISPD: Melt-pressed plaques with a thickness of ≈0.1 mm were placed on a grounded copper plate with a hot plate (PZ35 ET) underneath, while its upper surface was exposed to air. First, corona charging of the sample surface was done via a needle (hemispherical tip with a diameter of 0.95 mm) and a grid electrode between the needle and the sample (90×90 mm^2), both mounted on a fixed arm and connected to DC voltage supplies (Kyoritsu KM-106, ± 15 kV). The surface-to-grid and needle-to-grid distances were 5 and 3 mm, respectively. Upon completion of the charging step, the center of the sample was placed under a Kelvin type electrostatic probe (Trek PN 6000B) connected to an electrostatic voltmeter (Trek 347). The surface potential was measured by the electrostatic voltmeter at a rate of 1 reading per second employing a data acquisition card connected to a PC.

Supporting Information

Supporting Information is available from the Wiley Online Library or from the author.

Acknowledgements

The authors gratefully acknowledge the Swedish Foundation for Strategic Research (Grant Agreement No. FFL15-0147), The Knut and Alice Wallenberg Foundation through the project "Mastering Morphology for Solution-borne Electronics" as well as Chalmers' Area of Advance Energy for funding.

Conflict of Interest

The authors declare no conflict of interest.

Data Availability Statement

The data that support the findings of this study are available from the corresponding author upon reasonable request.

Keywords

conjugated polymers, electrical conductivity reducing additives, high-voltage direct-current (HVDC) insulation, low-density polyethylene (LDPE), poly(3-hexylthiophene) (P3HT)

Received: January 27, 2021
Revised: April 7, 2021
Published online:

[1] *P3HT Revisited – From Molecular Scale to Solar Cell Devices* (Ed: S. Ludwigs), Vol. *265*, Springer, Berlin, Germany **2014**.
[2] *Nanostructured Materials for Type III Photovoltaics* (Eds: P. Skabara, M. A. Malik), Royal Society of Chemistry, London, UK **2017**.
[3] A. Lund, Y. Wu, B. Fenech-Salerno, F. Torrisi, T. Carmichael, C. Müller, *MRS Bull.* **2021**, https://doi.org/10.1557/s43577-021-00117-0.
[4] S. Goffri, C. Müller, N. Stingelin-Stutzmann, D. W. Breiby, C. P. Radano, J. W. Andreasen, R. Thompson, R. A. J. Janssen, M. M. Nielsen, P. Smith, H. Sirringhaus, *Nat. Mater.* **2006**, *5*, 950.
[5] L. Z. Qiu, X. Wang, W. H. Lee, J. A. Lim, J. S. Kim, D. Kwak, K. Cho, *Chem. Mater.* **2009**, *21*, 4380.
[6] E. Song, B. Kang, H. H. Choi, D. H. Sin, H. Lee, W. H. Lee, K. Cho, *Adv. Electron. Mater.* **2016**, *2*, 1500250.
[7] A. D. Scaccabarozzi, J. I. Basham, L. Yu, P. Westacott, W. Zhang, A. Amassian, I. McCulloch, M. Caironi, D. J. Gundlach, N. Stingelin, *J. Mater. Chem. C* **2020**, *8*, 15406.
[8] T. A. M. Ferenczi, C. Müller, D. D. C. Bradley, P. Smith, J. Nelson, N. Stingelin, *Adv. Mater.* **2011**, *23*, 4093.
[9] B. A. Nieto-Diaz, C. Pearson, Z. Al-Busaidi, L. Bowen, M. C. Petty, C. Groves, *Sol. Energy Mater. Sol. Cells* **2021**, *219*, 110765.
[10] G. H. Lu, L. J. Bu, S. J. Li, X. N. Yang, *Adv. Mater.* **2014**, *26*, 2359.
[11] D. Kiefer, L. Y. Yu, E. Fransson, A. Gomez, D. Primetzhofer, A. Amassian, M. Campoy-Quiles, C. Müller, *Adv. Sci.* **2017**, *4*, 1600203.
[12] G. C. Montanari, P. H. F. Morshuis, M. Zhou, G. C. Stevens, A. S. Vaughan, Z. Han, D. Li, *High Voltage* **2018**, *3*, 90.
[13] A. Alassi, S. Bañales, O. Ellabban, G. Adam, C. MacIver, *Renewable Sustainable Energy Rev.* **2019**, *112*, 530.
[14] A. M. Pourrahimi, R. T. Olsson, M. S. Hedenqvist, *Adv. Mater.* **2018**, *30*, 1703624.
[15] M. G. Andersson, J. Hynynen, M. R. Andersson, V. Englund, P.-O. Hagstrand, T. Gkourmpis, C. Müller, *ACS Macro Lett.* **2017**, *6*, 78.
[16] A. M. Pourrahimi, T. A. Hoang, D. Liu, L. K. Pallon, S. Gubanski, R. T. Olsson, U. W. Gedde, M. S. Hedenqvist, *Adv. Mater.* **2016**, *28*, 8651.
[17] L. K. H. Pallon, A. T. Hoang, A. M. Pourrahimi, M. S. Hedenqvist, F. Nilsson, S. Gubanski, U. W. Gedde, R. T. Olsson, *J. Mater. Chem. A* **2016**, *4*, 8590.
[18] D. Liu, A. T. Hoang, A. M. Pourrahimi, L. K. H. Pallon, F. Nilsson, S. M. Gubanski, R. T. Olsson, M. S. Hedenqvist, U. W. Gedde, *IEEE Trans. Dielectr. Electr. Insul.* **2017**, *24*, 1396.
[19] K. Y. Lau, A. S. Vaughan, G. Chen, I. L. Hosier, A. F. Holt, *J. Phys. Conf. Ser.* **2013**, *472*, 012003.
[20] F. Nilsson, M. Karlsson, U. Gedde, R. Kádár, K. Gaska, C. Müller, P.-O. Hagstrand, R. Olsson, M. Hedenqvist, T. Gkourmpis, *Composites, Part B* **2021**, *204*, 108498.
[21] J. S. Park, Y. S. Kim, H.-J. Jung, D. Park, J. Y. Yoo, J. H. Nam, Y. J. Kim, *J. Nanomater.* **2019**, *2019*, 9035297.

[22] B. X. Du, C. Han, J. Li, Z. Li, *IEEE Trans. Dielectr. Electr. Insul.* **2020**, *27*, 418.
[23] Y. Yamano, M. Iizuka, *IEEE Trans. Dielectr. Electr. Insul.* **2009**, *16*, 189.
[24] X. Chen, A. Paramane, H. Liu, J. Tie, Z. Wei, Y. Tanaka, *Polym. Eng. Sci.* **2020**, *60*, 717.
[25] B. Du, C. Han, Z. Li, J. Li, *IEEE Access* **2019**, *7*, 66576.
[26] H. Yan, J. G. Manion, M. J. Yuan, F. P. G. de Arquer, G. R. McKeown, S. Beaupre, M. Leclerc, E. H. Sargent, D. S. Seferos, *Adv. Mater.* **2016**, *28*, 6491.
[27] M. L. Tietze, P. Pahner, K. Schmidt, K. Leo, B. Lussem, *Adv. Funct. Mater.* **2015**, *25*, 2701.
[28] S. Kumara, X. Xu, T. Hammarström, Y. Ouyang, A. M. Pourrahimi, C. Müller, Y. V. Serdyuk, *Energies* **2020**, *13*, 1434.
[29] J. Clark, C. Silva, R. H. Friend, F. C. Spano, *Phys. Rev. Lett.* **2007**, *98*, 206406.
[30] F. Paquin, H. Yamagata, N. J. Hestand, M. Sakowicz, N. Bérubé, M. Côté, L. X. Reynolds, S. A. Haque, N. Stingelin, F. C. Spano, C. Silva, *Phys. Rev. B* **2013**, *88*, 155202.
[31] D. Raithel, S. Baderschneider, T. B. de Queiroz, R. Lohwasser, J. Köhler, M. Thelakkat, S. Kümmel, R. Hildner, *Macromolecules* **2016**, *49*, 9553.
[32] J. Clark, J.-F. Chang, F. C. Spano, R. H. Friend, C. Silva, *Appl. Phys. Lett.* **2009**, *94*, 163306.
[33] M. J. Dyson, E. Lariou, J. Martin, R. Li, H. Erothu, G. Wantz, P. D. Topham, O. J. Dautel, S. C. Hayes, P. N. Stavrinou, N. Stingelin, *Chem. Mater.* **2019**, *31*, 6540.
[34] V. Adamec, J. H. Calderwood, *J. Phys. D: Appl. Phys.* **1981**, *14*, 1487.
[35] M. Mauri, A. I. Hofmann, D. Gómez-Heincke, S. Kumara, A. M. Pourrahimi, Y. Ouyang, P.-O. Hagstrand, T. Gkourmpis, X. Xu, O. Prieto, C. Müller, *Polym. Int.* **2020**, *69*, 404.
[36] G. Mazzanti, M. Marzinotto, *Space Charge in HVDC Extruded Insulation: Storage, Effects, and Measurement Methods*, John Wiley & Sons, Inc, Hoboken, NJ, USA **2013**.
[37] T. Mizutani, *IEEE Trans. Dielectr. Electr. Insul.* **1994**, *1*, 923.
[38] Y. Wang, M. Hao, Z. Xu, D. Qiang, G. Chen, A. Vaughan, *Appl. Phys. Lett.* **2018**, *113*, 022904.
[39] G. C. Montanari, D. Fabiani, *IEEE Trans. Dielectr. Electr. Insul.* **2000**, *7*, 322.
[40] A. Merdasa, A. Kiligaridis, C. Rehermann, M. Abdi-Jalebi, J. Stöber, B. Louis, M. Gerhard, S. D. Stranks, E. L. Unger, I. G. Scheblykin, *ACS Energy Lett.* **2019**, *4*, 1370.
[41] X. Xu, M. Karlsson, K. Gaska, S. Gubanski, H. Hillborg, U. Gedde, *Proc. Nordic Insulation Symp.*, Västerås, Sweden, June **2017**.
[42] T. Maeno, T. Futami, H. Kushibe, T. Takada, C. M. Cooke, *IEEE Trans. Electr. Insul.* **1988**, *23*, 433.